

*Refereed Proceedings*  
*Separations Technology VI: New Perspectives*  
*on Very Large-Scale Operations*

---

Engineering Conferences International

Year 2004

---

The Superior Aspects of an Arc  
Downcomer Tray with Total Deflectors

ZhiBing Zhang\*

WeiMing Meng<sup>†</sup>

Zhen Zhou<sup>‡</sup>

YinChun Liang\*\*

\*Separation Engineering Research Center, SERC, Nanjing University, Nanjing, 210093, P.R.C., [segz@nju.edu.cn](mailto:segz@nju.edu.cn)

<sup>†</sup>Separation Engineering Research Center, SERC, Nanjing University, Nanjing, 210093, P.R.C.

<sup>‡</sup>Separation Engineering Research Center, SERC, Nanjing University, Nanjing, 210093, P.R.C.

\*\*Separation Engineering Research Center, SERC, Nanjing University, Nanjing, 210093, P.R.C.

This paper is posted at ECI Digital Archives.

[http://dc.engconfintl.org/separations\\_technology\\_vi/6](http://dc.engconfintl.org/separations_technology_vi/6)

# THE SUPERIOR ASPECTS OF AN ARC DOWNCOMER TRAY WITH TOTAL DEFLECTORS

ZhiBing Zhang, WeiMing Meng, Zhen Zhou and YinChun Liang

Separation Engineering Research Center, SERC

Nanjing University, Nanjing, 210093, P.R.C.

T: 86-25-8359-3772 F: 86-25-8620-7044 E: segz@nju.edu.cn

## ABSTRACT

A new structural tray — the arc downcomer tray with total deflectors (ADTTD) was designed based on the numerical calculation of entropy generation rate. A pilot-scale setup was established to evaluate its hydrodynamics, heat transfer and mass transfer performances. The correlations for calculating the tray pressure drop and downcomer backup were derived. The measured temperature profiles of the liquid layer on the tray show that the flow pattern is nearly in an ideal mode if suitable deflectors are designed. The pressure drop of this tray decreases by approximately 50% compared with that of a conventional sieve tray in the region of intermediate to high vapor load. The liquid-phase Murphree tray efficiency of the tray is almost 30% higher than that of the traditional sieve tray under the same operating conditions. The weeping curve of the tray was also found to be a little lower than that of conventional trays. Experiments and industrial applications demonstrated that the ADTTD had some important advantages in lower pressure drop and energy-consumption, higher capacity and tray efficiency over the conventional sieve trays.

## 1. INTRODUCTION

Trays have been the dominant tower internals because of their reliability, good plugging resistance, good corrosion resistance, and higher efficiency at elevated pressure, etc. Traditional trays, however, have some disadvantages as well, such as higher pressure drop, and low capacity. Based on new design concepts in the past 10 years, new trays, such as the Nye tray of the Glitsch Company<sup>1</sup> and the MD tray of the UOP Company,<sup>2</sup> have been developed and used successfully in industrial processes.

In our laboratory a novel structural tray—ADTTD was designed based on the numerical calculation of entropy generation rate (EGR) for a tray<sup>3</sup>. The hydrodynamic performance of this new tray was evaluated on a pilot device.<sup>7</sup>

This work will give an overall description of the design criteria of ADTTD from the calculation of EGR, followed by the further study on its performance, including liquid

flow pattern on the tray, temperature profile of the liquid layer, and Murphree tray efficiency, etc.

## 2. FUNDAMENTALS OF THE DESIGN CRITERIA OF ADTTD

Distillation processes with low energy demand have been generated using various kinds of thermodynamic analysis methods<sup>4</sup>. In all these methods, the analysis and calculation of the entropy generation rate (EGR) within a tray and/or a column are the key points to address in designing new distillation processes or mass-transfer elements. In our laboratory, a new model was developed, focusing on the effects of structural parameters of a tray on the process EGR.

According to non-equilibrium thermodynamics, for the case of non-viscous fluids with no chemical reactions and no external forces exerted on a system of N species at constant pressure, the EGR per unit volume,  $\sigma$ , can be written as

$$\sigma = -J_q \frac{\nabla T}{T^2} - \frac{1}{T} \sum_{i=1}^N J_i \nabla \mu_{i,T}^c \quad (1)$$

where the contribution of temperature variation to the chemical potential gradient ( $\nabla \mu$ ) of component  $i$  is neglected.  $J_q$  and  $J_i$  are the heat and mass fluxes, respectively. By applying the mechanical balance equation and the Gibbs-Duhem equation in Equation (1), a general working equation of EGR for a multi-component system can be derived as

$$\sigma = -J_q \frac{\nabla T}{T^2} - \frac{1}{T} \sum_{i=1}^{N-1} J_i \left[ \sum_{k=1}^{N-1} \left( \delta_{ik} + \frac{M_i y_k}{M_N y_N} \right) \nabla \mu_{k,T} \right] \quad (2)$$

where  $M$ ,  $y$  and  $\delta$  are molecular weight, mole fraction and  $\delta$  function, respectively. It is very hard to apply Equation (2) to calculate the EGR for a multi-component system. However, for a binary system, Equation (2) can be simplified, based on the following four assumptions: (1) there is no significant pressure gradient along or across the vapor-liquid interface film and the liquid phase is well distributed on a stage; (2) the temperature and chemical potential gradients are constant in the vapor phase on each stage, and the temperature gradient along the column is small; (3) the thermal contribution to the mass fluxes is negligible; and (4) the dissipation of energy is attributed mainly to the mass transfer across the interface layer with a thickness of  $\Delta x$  ( $=D/k_c$ ) and a constant area of  $a$ . Thus, by using the linear phenomenological relationship of non-equilibrium thermodynamics and applying the Onsager reciprocity relations to the fluxes  $J_q$  and  $J_i$ , a simplified expression for the total EGR,  $P$ , in a stage was obtained after mathematical derivation:

$$P = \int_0^v \sigma dv = \frac{\Delta \mu_l}{T m_h} k_c a \Delta c_l \quad (3)$$

where  $m$  is the mass fraction, and the subscripts  $l$  and  $h$  denote the light and heavy

components, respectively.

The relationship between the tray parameters and the EGR in a distillation column was simulated for the binary benzene – toluene system based on Equation (3) for the calculation of EGR and the AIChE equation<sup>5</sup> for the stage efficiency. From the calculations, four important and interesting findings relating the tray structure to the EGR were obtained. (1) Increasing the tray diameter causes a higher EGR on a tray under identical operating conditions, due to the decreased hole velocity and increased active hole area with increasing tray diameter. The decreased height of the liquid over the weir when increasing the tray diameter can reduce somewhat the EGR on a tray, but it is not a dominant factor. (2) A higher weir height causes higher tray efficiency and higher tray pressure drop that induce both positive and negative effects on the EGR. The calculation showed that the EGR increased with increasing weir height since the increased pressure drop was the primary factor. (3) A decrease in weir length leads to an increasing EGR. EGR profiles change less with variation of weir length than with variation of weir height. (4) Increasing active area of tray can noticeably reduce the EGR, mainly due to the decreased tray pressure drop and the increased mass transfer efficiency that both result from the larger active area.

The above four findings provide a design criteria for the development of new trays. In our laboratory, a novel tray, ADTTD, was thus designed and is shown in Figure 1. This tray consists principally of three parts: a specially designed crescent downcomer<sup>6</sup>, sieve or valve tray, and total deflectors. The weir is also in the form of a crescent. This design offers the advantages of (1) a reduction in the hole vapor flow velocity because of the increase in active area, leading to a decrease in entrainment so that the tray spacing can be shortened and the capital investment for the column reduced; (2) decreases in both the pressure drop for these trays and the flooding in the downcomer because of the low vapor velocity; and (3) a lengthening of the fluid flow path and regulated liquid flow pattern because of the tray structure, so that the contacting time for liquid-vapor is longer than that in conventional trays. Liquid backmixing is reduced by the use of the total deflectors. Therefore ADTTD can have higher efficiency and higher capacity. For revamping, ADTTD can provide higher capacity without the expense of installing the additional trays that are usually required to compensate for reduced tray efficiency. Even the original tower attachments can most likely be reused. ADTTD is able to achieve the required capacity and efficiency for a new tower in reduced sizes (diameter and height). A comparison of the EGR on the tray and on a conventional sieve tray of the same tray spacing, diameter and weir height was performed showing that ADTTD is able to reduce the EGR by 30%. It has the characteristics of energy-saving, large capacity and high separation efficiency.

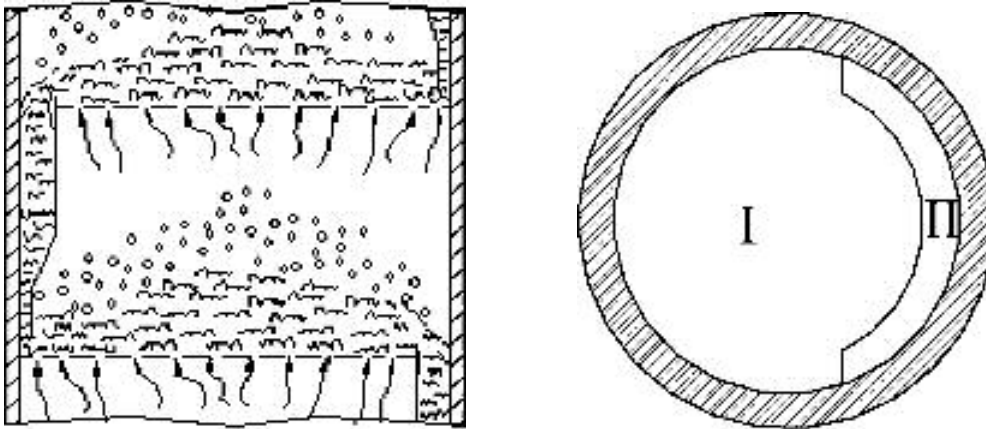


**Figure 1.** Schematic view of ADTTD.

### 3. EXPERIMENTAL SECTION

A schematic diagram of the experimental apparatus is shown in Figure 2. Three identical trays were placed in a column with a diameter of 1000 mm. The middle tray served as a test tray, the upper tray functioned as a stabilizing tray, and the bottom tray played the role of evenly distributing vapor. The space between each pair of adjacent trays was 500 mm. The tray structural parameters were as follows: hole diameter of 11 mm; weir length of 714 mm; weir heights of 21, 35, and 42 mm; total hole area over the tray area of 10.5%; and downcomer exit of 50 mm.

Air/water was taken as the operating system, with a vapor velocity range of 0.6-3.5 m s<sup>-1</sup> and a liquid flow rate range of 4.0-32 m h<sup>-1</sup>. The pressure drop for the tray was measured by a "U" pressure differential meter, and the downcomer liquid backup was measured by a liquidometer. The flow pattern was determined with soft colored silks and potassium permanganate as a tracer, the vapor rate was measured with a probe flowmeter of type SY-93 manufactured by EPI company, USA and the liquid with a smart vortex flowmeter 8800C supplied by Fisher-Rosemount Co. Ltd. (Shanghai).

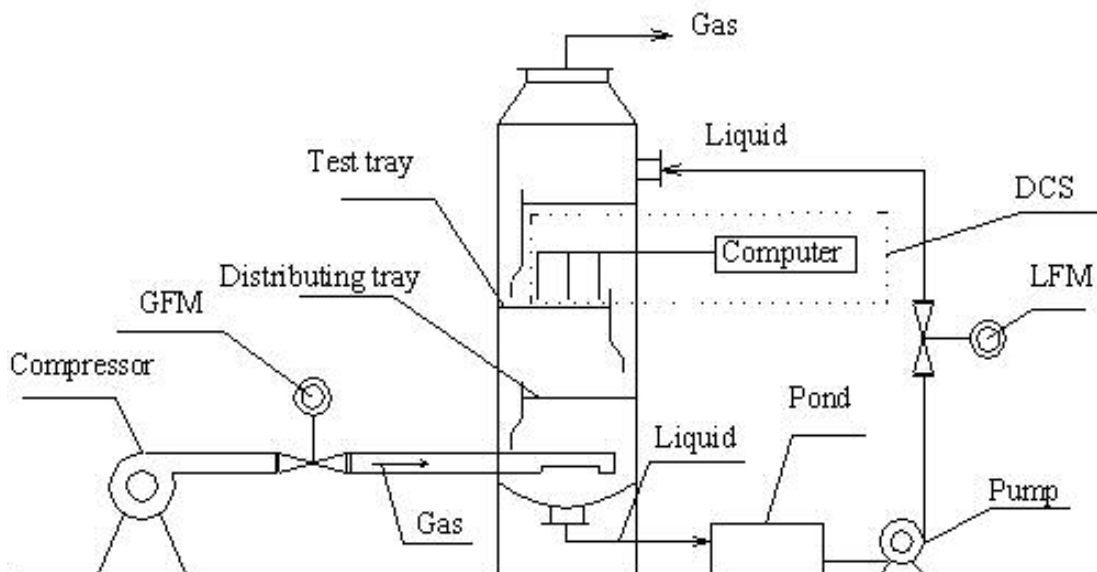


**Figure 2.** Schematic diagram of the experimental apparatus

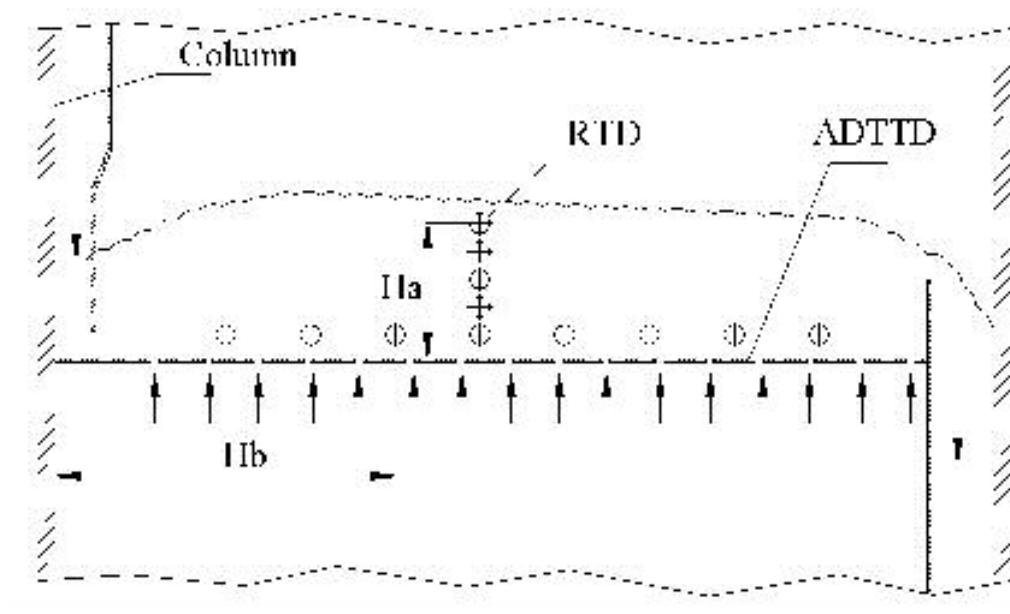


**Figure 3.** Positions of RTDs;

**Ha**, distance from the testpoint of the RTD to the tray surface, equal to the height of the liquid layer; **Hb**, distance from the testpoint to the liquid inlet.

Temperatures within the liquid layer on trays were determined by sensitive platinum resistive thermal detectors (RTDs), specially designed with an accuracy of  $\pm 0.01$  °C. The positioning of the RTDs is shown in Figure 3. Desorption tests of oxygen from the water were carried out to measure  $E_{ML}$  (it is unadvisable to measure  $E_{MV}$  because the oxygen desorption process is controlled by the liquid film). The oxygen-rich water was prepared by injecting oxygen into the water at the water source. Enough time was needed to let oxygen dissolve sufficiently into the water so that an oxygen content of

about 20 mg/L (O<sub>2</sub>/H<sub>2</sub>O) was obtained. When the testing system reached a steady state, liquid samples were collected from the inlet and outlet of the tray at the same time. Then oxygen contents were titrated without delay by iodometry.

#### 4. RESULTS AND DISCUSSION

**4.1 Flow Patterns on the Tray.** The flow patterns on the tray for various liquid flowrates were studied for liquid-only flow and a liquid-vapor biphas flow at three weir heights (21, 35, 42mm). The liquid flow on the tray without deflectors can be divided into two parts: (□) an eddy zone and (□) a bulk flow zone. The main reason for the eddy zone is that the liquid outflow from the downcomer has a tendency to flow toward the center of the tray, which results in a maldistribution of the liquid on the tray and an eddy near the column wall. It was found that the overflow rate had a remarkable effect on the liquid flow pattern and that the area of the eddy zone was enlarged with increasing liquid flow rate. The area of the eddy for biphas flow increased slowly with an increment of flux and is smaller than that for single-phase flow. The higher weir height has little influence on the single-phase flow pattern, but remarkably, does influence the eddy area for biphas flow.

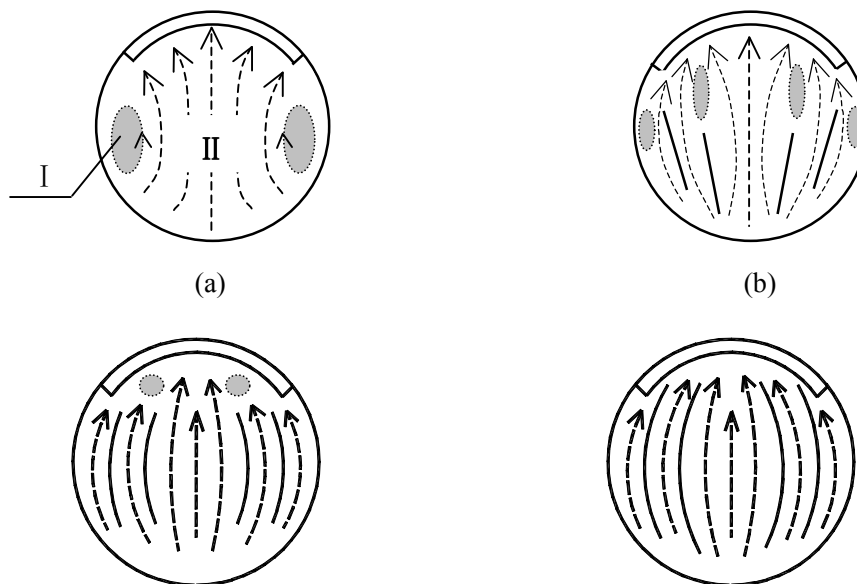


**Figure 4.** Flow patterns on trays  
 (a) with no deflectors, (b) with short deflector #1;  
 (c) with longer deflectors #2, (d) with total deflectors #3.

**Table 1. Specifications of Deflectors**

number	length (mm)	height (mm)	form
#1	200	40	line
#2	600	50	arc
#3	800	50	arc

To reduce the eddy zone and to optimize the flow pattern, deflectors were placed on

the tray to regulate and distribute the flow. Figure 4a-d show the flow patterns without and with the deflectors, respectively. The eddy zone can be reduced when deflector #1 is used, but there is some small backflow on the tray. The eddy area almost disappears when deflector #2 is used, and the flow pattern is approximately in a plug state when the deflector #3 is installed. Specifications of the deflectors are given in Table 1.

In the following tests, deflector #3 was adopted and its length was increased to achieve a "full-guide" from the inlet to the overflow weir, which was expected to completely divide the tray surface area into several individual channels. Deflectors were arranged like the meridians of the globe on two-dimensional maps. Coming from the inlet, the liquid was evenly guided into these channels. The liquid vortex and backflow were almost eliminated since the velocity gradient of crossflow was basically reduced in each channel. Thus plug flow (an ideal flow pattern) was expected and a multi-plug flow pattern could be set up. The same method can be applied to other round-shaped trays such as valve trays and all conventional sieve trays.

**4.2 Pressure Drop.** Compared with a conventional sieve tray, the pressure drop for ADTTD is greatly reduced due to its larger vapor flow area. It allows more area to be perforated and the hole vapor velocity is then lower than that of the conventional tray for an identical vapor flow rate, resulting in a lower dry tray pressure drop across the tray (see Figure 5). The equation for the pressure drop per tray of ADTTD was obtained by modifying the discharge coefficient in the formula for conventional trays

$$h_d = 0.051 (\rho_v/\rho_L) [u_o / (k C_o)]^2 \quad (4)$$

Equation (4) is consistent with experimental results as shown in Figure 5. The pressure drop per tray increases with increasing liquid flow rate  $F$  factor at a fixed weir height of 42 mm (Figure 6, 8), and weir height at an fixed liquid flow rate (Figure 7). Figure 5 shows that the per tray pressure drop of the ADTTD is almost one-half of that of a conventional tray in the range of medium to high vapor flow rates. The divergence of the pressure drop per tray between the two trays increases with increasing vapor flow rate, as shown in Figure 6. As in other trays, the pressure drop of ADTTD depends on the pressure drop per dry tray and the clear liquid height on the tray,

$$h_t = h_d + h_l \quad (5)$$

$$h_l = \xi\beta(h_w + h_{ow}) \quad (6)$$

where  $h_l$  in Equation (6) was obtained on the basis of conventional methods with some modifications. The calculations show that these equations fit with the experiments (Figure 6) and the divergence in the pressure drop per tray between the ADTTD tray and a conventional one comes mainly from the differences in the pressure drop per dry tray.



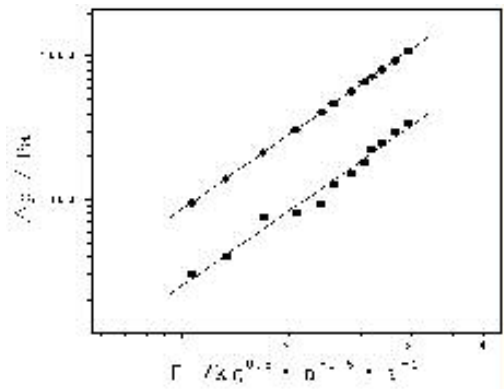


**Fig.5** Pressure drop per dry tray at different F-factors flow-rates

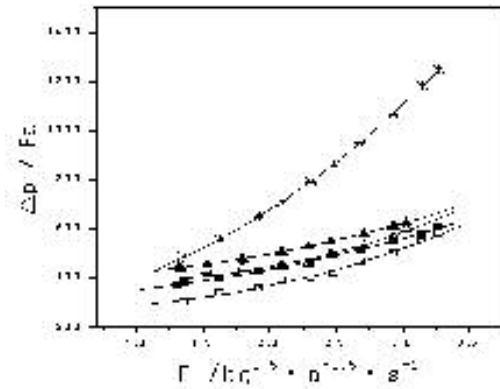


**Fig.6** Pressure drop per tray at different liquid flow-rates

( $\phi=10.5\%$ ,  $d_0=11\text{mm}$ ,  $h_w=21\text{mm}$ )

● traditional sieve tray; ■ ADTTD

▲ cal.

■ cal.

( $\phi=10.5\%$ ,  $d_0=11\text{mm}$ ,  $h_w=42\text{mm}$ )

$L=5.7\text{m}^3\cdot\text{h}^{-1}$ ; + traditional sieve tray; ADTTD Δ exptl

$L=15.5\text{m}^3\cdot\text{h}^{-1}$ ; ADTTD □ exptl.;

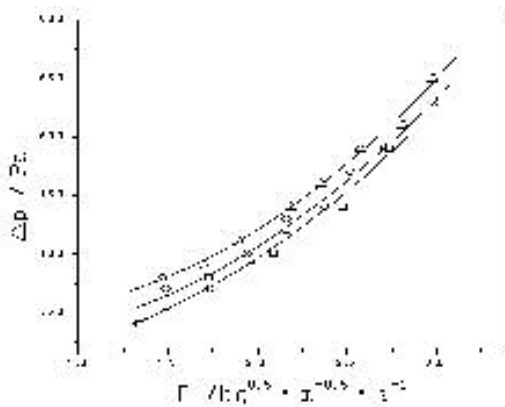


**Fig.7** Effect of weir height on pressure drop

( $\phi=10.5\%$ ,  $d_0=11\text{mm}$ ,  $L=11.9\text{m}^3\cdot\text{h}^{-1}$ , ADTTD)

$h_w/\text{mm}$ : □ 21; ○ 35; Δ 42

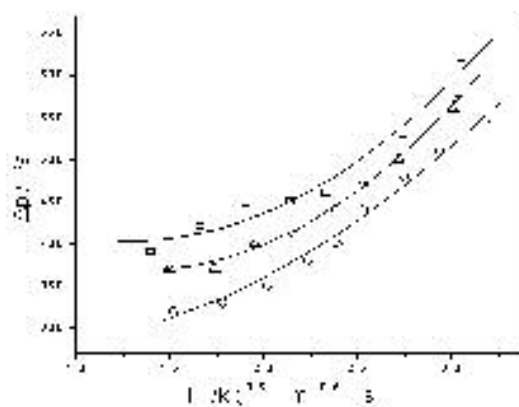


**Fig.8** Effect of liquid flow-rate on pressure drop

( $\phi=10.5\%$ ,  $d_0=11\text{mm}$ ,  $h_w=35\text{mm}$ , ADTTD)

$L/\text{m}^3\cdot\text{h}^{-1}$ : ◇ 5.4; Δ 11.9; □ 17.5

**4.3 Downcomer Backup.** The downcomer liquid backup can be calculated from Equation 7 in terms of the mechanical energy balance equation

$$h_d = h_t + h_l + h_{dc} \quad (7)$$

where  $h_{dc}$  is the head loss in the downcomer that is attributed to the downcomer exit restriction;  $h_l$  is the clear liquid height on the tray.  $h_l = h_w + h_{ow}$  if  $h_w + h_{ow} \gg 0.05\text{m}$ ; otherwise  $h_l = 0.05\text{m}$ . The relation between  $h_{dc}$  and  $L_s$  can be deduced from the Bernoulli equation

$$h_{dc} = 0.051 [ L_s / (C_d S) ]^2 \quad (8)$$

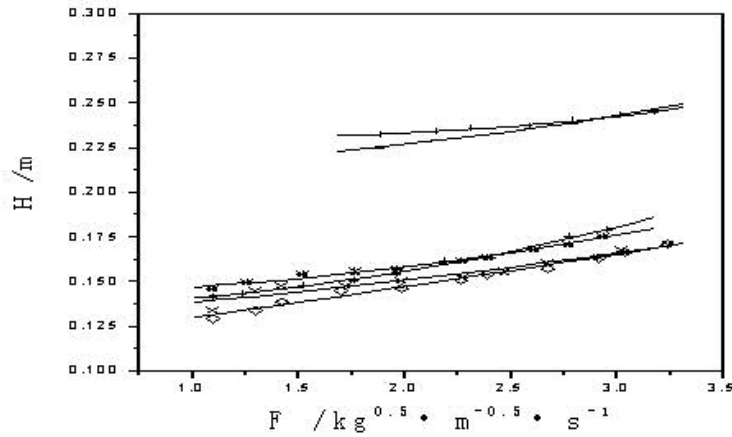


**Figure 9.** Effect of F-factor on liquid height in the downcomer.  
 ( $\phi=10.5\%$ ,  $d_0=11\text{mm}$ ,  $L=9.2\text{m}^3\cdot\text{h}^{-1}$ ): ■ ■  $s_1$  exptl.; +  $s_1$  cal; ◇  $s_2$  exptl; ×  $s_2$  cal.  
 ( $\phi=10.5\%$ ,  $d_0=11\text{mm}$ ,  $L=18.2\text{m}^3\cdot\text{h}^{-1}$ ): -  $s_1$  exptl; +  $s_1$  cal.

The downcomer backup values were measured at areas of 0.2784 and 0.428 m<sup>2</sup>. The calculated data using Equation 8 differed from the experiments by less than 10%, as shown in Figure 9. The downcomer backup increases with increasing vapor flow rate and decreasing exit area. The most influential factor for downcomer backup is the liquid flow rate.  $h_d$  goes up dramatically as the liquid flow rate increases when other operating parameters are kept constant.

**4.4 Temperature Profile of the Liquid Layer.** Test results are presented in Figure 10 and 11. Figure 10 shows the vertical temperature profile in the liquid layer of the tray that tends to decrease linearly as the liquid layer height increases. If the flow pattern is plug flow, the theoretical deduction leads to

$$T = -b_1Kh + b_2, \tag{9}$$

where  $T$  is the temperature of the liquid layer,  $h$  is the height of the same layer, and  $b_1$ ,  $K$ ,  $b_2$  are constants. Since the experimental results agree well with Equation (9), it can be deduced that the flow pattern on the tray is plug flow, the same as what we have seen in flow pattern experiments in Fig. 4d. Figure 11 shows the temperature profile along the liquid flow channel in the horizontal direction. At the same height of liquid layer, the temperature also increases linearly from the liquid inlet to the outlet,

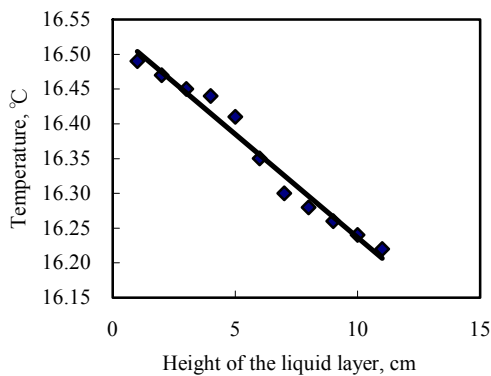


**Figure 10.** Vertical temperature profile of the liquid layer on 95 tray

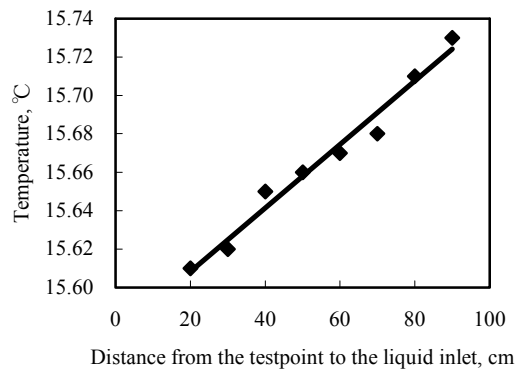


**Figure 11.** Horizontal temperature profile of the liquid layer on 95 tray

indicating an ideal flow pattern being reached on the tray.

**4.5 Murphree Tray Efficiencies.** The efficiencies of the ADTTD tray and a traditional sieve tray are compared in Figure 12. The efficiency of the former is about 30% higher than that of the latter under the same operating conditions.  $E_{ML}$  of the ADTTD tray is more stable with F factor than that of traditional sieve tray, and the ADTTD tray has a higher capacity and operating flexibility than the traditional sieve tray.

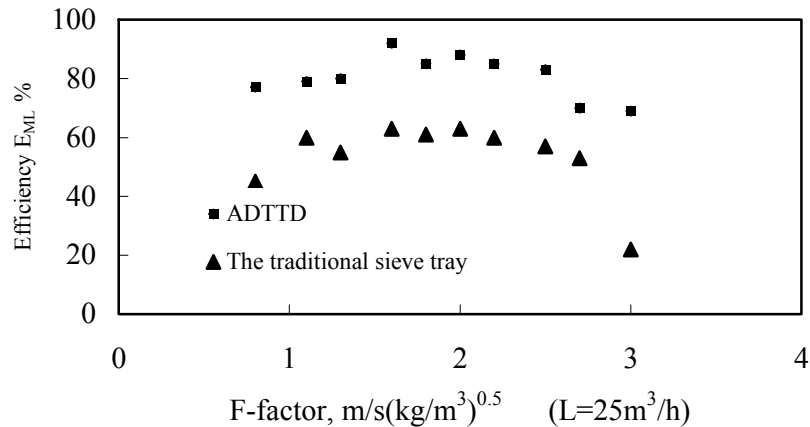


**Figure 12.** Tray efficiencies of 95-II tray and traditional sieve tray at different gas-phase F-factors

## 5. APPLICATIONS OF ADTTD

### Revamping of Dehydration Column for Acetic Acid / Water System

The dehydration column for the acetic acid / water system is located in Yizheng Chemical Fiber Co.Ltd. of SINOPEC Group, on the bank of Yangtze River, and originally designed by Glitsch Company for the recovery of the chemical solvent acetic acid in the process of PTA (p-phthalic acid ) manufacture. The capacity of equivalent to 100% purity acetic acid is 330 kt/ a . This tower has a height of more than 58000 mm with two sections, the upper one with a diameter of  $\phi 3200$  mm containing 77 conventional sieve trays and the lower one with a diameter of  $\phi 3500$  mm with 13 identical trays.

To meet the needs of PTA production capacity increase from 250 kt/a to 325 kt/a,- an improvement of 30% - the capacity of the column has to be accordingly increased up to 430 kt/ a.

The restrictions for the revamping given by the owner were:

- (1) keep the height and diameter of the column constant,
- (2) keep the heat transfer area of the reboiler constant,
- (3) keep the locations and pipe diameters of four feed points, product exit and manhole position,

(4) keep the total expenses of the revamping lower than 5 million RMB (about 0.6 million USD).

The specifications of the project that should be reached according to the contract were:

- (1) the capacity of the column after revamping is not less than 430 kt/a (100% purity acetic acid equivalent),
- (2) the total pressure drop along the column has to be reduced from 87kPa before the revamping to 40kPa afterwards to follow the restriction (2) and meet the new needs of heat transfer in the reboiler,
- (3) the concentration of acetic acid in the vapor phase at the top has to be reduced to below 1.5%(mass) from 2.8%(mass) on average before the operation. The concentration of acetic acid in the liquid phase at the bottom must be kept to 95%(mass) in average.
- (4) the period of the revamping (from simulation to installation and to start-up ) to be not more than 60 days.

As the bid winner, SERC (Separation Engineering Research Center, Nanjing University) redesigned this tower by using non-wall flow structured Sionpak packing in the upper section and 13 ADTTD trays in the lower section to replace 90 conventional sieve trays. Non-wall flow structured Sionpak packing was developed and patented in 1996, and the ADTTD tray in 1997. The most significant difficulties encountered in the revamping were the separation efficiency and the total pressure drop of the packings and trays under high vapor load. The maximum F factor of the packing section is as high as 3.0 and the tray section has a liquid load of 9-25m<sup>3</sup>/ m<sup>2</sup>. h. A serious Marangoni effect in the packed section was also a barrier to packings giving good separation efficiency.

The operating results after the revamping showed that the capacity of the dehydration system was increased by 33%, the total pressure drop was down to 44 kPa which implied that no more heat transfer area was needed in the reboiler for the new capacity. And finally the concentration of acetic acid in the vapor phase at the top was reduced to below 1.3% (mass) on average which indicated that total efficiency of the column was remarkably improved.

Until now, the revamped column has been satisfactorily operated for 6 years at a capacity of 439 kt /a (100% purity acetic acid equivalent)

## 6. CONCLUSIONS

The following conclusions can be drawn from this study:

- (1) The ADTTD tray was designed based on the thermodynamic analysis of the entropy generation rate on the trays;
- (2) The ADTTD tray offers the advantages of a lower pressure drop and bigger

- capacity than a conventional tray;
- (3) The flow pattern on a ADTTD tray without deflectors is similar to that on a conventional tray, and it can be greatly improved to an almost ideal state by installing suitable deflectors. The temperature profiles of the liquid layer on the tray are linear in the vertical and horizontal directions;
  - (4) The structural parameters of the ADTTD tray, except the downcomer, can be designed in a manner similar to conventional trays, but with some modification of the equation for calculating the dry tray pressure drop and the downcomer backup;
  - (5) The liquid-phase Murphree tray efficiency of the ADTTD tray is almost 30% higher than that of the traditional sieve trays under the same operating conditions.

## NOMENCLATURE

$C_0$  = discharge coefficient

$C_d$  = flow coefficient

$E_{ML}$  = liquid phase Murphree tray efficiency

$h_d$  = pressure drop per dry tray

$h_{dc}$  = head loss in downcomer

$h_l$  = head of clear liquid on the tray

$h_w$  = weir height

$h_{ow}$  = weir crest

$L_S$  = liquid flow rate

$S$  = section area of downcomer outlet

$u_0$  = hole flow velocity

### Greek Letters

$\rho_L, \rho_v$  = densities of the vapor and the liquid, respectively

$\kappa$  = modified factor ( $\kappa=0.84$ )

$\beta$  = aeration factor

$\xi$  = modified factor ( $\xi=0.88$ ), which is obtained from the experiments in this study

## LITERATURE CITED

- (1) de Bruyn, G.; Gangriwala, H. A.; Nye, J. O. High-capacity Nye trays. *Inst. Chem. Eng. Symp. Ser.* **1972**, *128*, A509-517.
- (2) Kunesh, J. G.; Kister, H. Z.; Lockett, M. J.; Fair, J. R. Distillation: Still Towering over Other Options. *Chem. Eng. Prog.* **1995**, *91*(10), 43-53.
- (3) Liu, Q. L.; Li, P.; Xiao, J.; Zhang, Z. B. A New Method for Designing an Energy-Saving Tray and Its Hydrodynamic Aspects: Model Development and Simulation. *Ind. Eng. Chem. Res.* **2002**, *41*, 285-292.
- (4) Ratkje, S. K.; Sauar, E.; Hansen, E. M.; Lien, K.M.; Hafskjold, B. Analysis of EGRs for Design of Distillation Columns. *Ind. Eng. Chem. Res.* **1995**, *34*, 3001-3007.
- (5) AIChE. Bubble Tray Design Manual: Prediction of Fractionation Efficiency; AIChE: New York, **1958**.
- (6) Zhang, Z. B.; Zhao, J.; Bian, K. J. High performance trayed tower. *Chinese Patent* CN 97106964.6, **1997**.
- (7) Peng Li, Qing Lin Liu, Jian Xiao, and Zhi Bing Zhang, A New Method for Designing an Energy-Saving Tray and Its Hydrodynamic Aspects: Hydrodynamic Aspects of ADTTD trays, *Ind. Eng. Chem. Res.* **2002**, *41*, 293-296

(8)Zhen Zhou, Ying Chun Liang, and Zhi Bing Zhang, A New Method for Designing an Energy-Saving Tray and Its Hydrodynamic Aspects: Temperature Distribution and Efficiency of Deflected Tray-95, *Ind. Eng.Chem.Res.***2003**,*43*,2219-2222

**KEY WORDS**

ADTTD tray, hydrodynamic, energy-saving, temperature profile, Murphree tray efficiency, flow pattern